

Preparation of Amphiphilic Poly(L-lactide)-graft-Chondroitin Sulfate Copolymer Self-aggregates and Its Aggregation Behavior

Chih-Ta Lee, Ching-Ping Huang, and Yu-Der Lee*

Department of Chemical Engineering, National Tsing Hua University, 101, Section 2, Kuang Fu Road, Hsin Chu, Taiwan, 300, ROC

Received December 26, 2005; Revised Manuscript Received February 21, 2006

Novel polymeric amphiphilic copolymers were synthesized using chondroitin sulfate (CS) as a hydrophilic segment and poly(L-lactide) (PLLA) as a hydrophobic segment. Micelles of those copolymers were formed in an aqueous phase and were characterized by ^1H NMR spectra, fluorescence techniques, dynamic light scattering (DLS), atomic force microscopy (AFM), and confocal microscopy. Their critical aggregation concentrations (CAC) are in the range of 0.0043–0.0091 mg/mL at 25 °C. The partition equilibrium constants, K_v , of the pyrene probe in the aqueous solution were from 3.65×10^5 to 1.41×10^6 at 25 °C. The mean diameters of the micelles were below 200 nm, and their sizes were narrowly distributed. The AFM images revealed that the self-aggregates were spherical. Additionally, the CS_n -PLLA micelles can efficiently transport within the cells via endocytosis as observed from confocal microscopy.

Introduction

Polymeric micelles derived from a block copolymer in an aqueous phase have recently attracted much interest, because of not only their unique morphological behaviors, but also their potential applications in drug delivery.^{1–3} Analogous to surfactants of low molecular weights, various polymeric amphiphiles have a core–corona structure which contains a hydrophobic internal core and a hydrophilic corona. This amphiphilicity makes it possible for the block or graft copolymers to form micelles in aqueous solution so that the inner core can serve as a microcontainer for various substances. Therefore, interest in the design and characterization of novel amphiphilic copolymers^{4,5} and the use of modified water-soluble polymers to form micelles or micelle-like aggregates in an aqueous phase has been growing.^{6,7}

Amphiphilic copolymers are well-known to form micelle structures at much lower critical aggregation concentrations (CAC)⁸ than surfactants of low molecular weight. These amphiphilic copolymers are thermodynamically stable in physiological solution because of their low critical aggregation concentrations.⁹ Accordingly, the solubility of the micelles and the interaction of micelles with the external environment are determined by the chemical and physical nature of the hydrophilic outer shell.¹⁰ Micellar aggregates prepared from amphiphilic copolymers are very small. In particular, these small-size micelles can easily escape from renal exclusion and the reticuloendothelial system,¹¹ which makes them ideal for drug carriers. Moreover, nanosized particles permeate more effectively into endothelial cells in the vicinity of solid tumors.¹² Polymeric micelles composed of block copolymers have been intensively investigated as drug delivery vehicles because of such characteristic advantages as small size, thermodynamic stability, ability to dissolve hydrophobic molecules, ability to protect a bioactive drug from the host, and protection of the

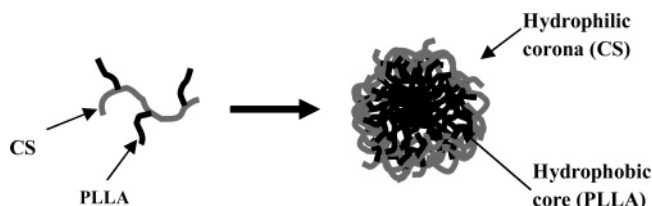


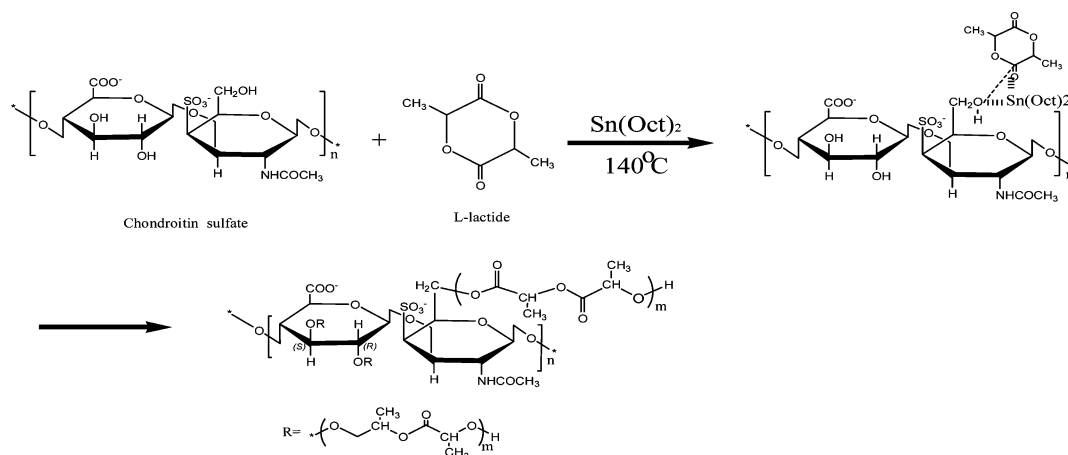
Figure 1. Schematic structure of nanoparticle of amphiphilic copolymer of chondroitin sulfate and poly(L-lactide) in an aqueous medium.

host against the toxicity of the drug.^{13,14} Natural polysaccharides, including dextran and heparin, have been modified with hydrophobic moieties, such as cholesteryl groups and alkyl chains, to form micelles and nanoparticles. For instance, Marie et al. synthesized chitosan-grafted copolymers via mini-emulsion to generate self-aggregates in an aqueous medium, and they are potential carriers for hydrophobic drugs.¹⁵

Chondroitin sulfate (CS) is a physiologically specific glycosaminoglycan (GAG). It is comprised of alternating units of β -1,3-linked glucuronic acid and (β -1,4) *N*-acetyl-galactosamine (GalNac) with sulfation at either the 4- or 6-position of GalNac.¹⁶ It is present mostly on the surface of the cells and in the extracellular matrix (ECM);¹⁷ it is the most abundant GAG molecule in the human body.

This study reports the synthesis and characterizations of self-aggregated amphiphilic CS_n -PLLA copolymers. These amphiphilic grafted copolymers with CS as the hydrophilic segment and PLLA as the hydrophobic segment could form micelles in aqueous milieu. Figure 1 schematically depicts the CS_n -PLLA micelles. The strategy for synthesizing CS_n -PLLA graft copolymers in this investigation may allow the preparation of polymeric biomimetic surfactants which can be used as drug carriers. These novel polymeric amphiphilic conjugates were physicochemically characterized by fluorescence techniques, dynamic light scattering, and atomic force microscopy. The specific cellular uptake behaviors of the flutamide-loaded micelles via endocytosis were examined by confocal scanning imaging as well.

* Corresponding author. Tel.: +886-3-571-3204. Fax: +886-3-571-5408. E-mail: ydlee@che.nthu.edu.tw.

Scheme 1. Reaction Scheme for the Synthesis of the Grafted Copolymers.

Experimental Section

Materials. L-Lactide was purchased from Lancaster and recrystallized twice from ethyl acetate, and then it was stored in a vacuum before use. Chondroitin sulfate (CS) (average $M_w = 12000$ g/mol, GPC, DMF) was obtained from Calbiochem and dried at a reduced pressure at 90°C under P_2O_5 for one night before use. Pyrene was obtained from Sigma Chemical Co. Stannous octoate (Sn(Oct)_2) was purchased from Sigma and used without further purification. Dimethyl sulfoxide (DMSO) (Aldrich Chemical Co., anhydrous), tetrahydrofuran (THF), ethyl acetate, hexane, and chloroform were used as received.

Synthesis of $\text{CS}_n\text{-PLLA}$ Graft Copolymers. The grafted copolymers of chondroitin sulfate/L-lactide ($\text{CS}_n\text{-PLLA}$) were prepared according to the method described by Donabedian and McCarthy¹⁸ (Scheme 1). Chondroitin sulfate was modified with L-lactide via ring-opening polymerization, and Sn(Oct)_2 was used as the catalyst. Chemical grafting of the PLLA chains onto chondroitin sulfate was expected to follow the initiation of the ring-opening polymerization by the hydroxyl functions of the chondroitin sulfate. Briefly, a 25-mL tri-neck flask with a reflux condenser was charged with different masses of L-lactide and chondroitin sulfate dissolved in a minimal amount (about 2 mL) of anhydrous DMSO. The flask was placed in an oil bath at 70°C in a vacuum to degas for around 40 min; then it was heated in another oil bath of 140°C for about 15 min, and 0.01 wt % of the Sn(Oct)_2 catalyst was injected. The reaction was continued for another 3 h. After the polymerization time, the product was cooled to room temperature. The reaction mixture was recovered and dialyzed against demineralized water. Various nonsolvents were used to recover the polymers, depending upon the extent of modification of CS. Copolymers with a large amount of lactide modification are insoluble in water, and the products were extracted with an ethyl acetate/water (6:4) mixture. The products were further purified to remove any unreacted monomer and poly(L-lactide) homopolymer that might have formed. The unreacted L-lactide monomer was extracted (with a Soxhlet device for 24 h) twice with hexane, and the PLLA homopolymer was removed by washing in toluene. Finally, the copolymer was precipitated in hexane and was dried in a vacuum (1 mmHg) at 40°C for 24 h.

^1H NMR Spectroscopy and Thermal Analysis. The ^1H NMR spectra of the copolymers were obtained using a 500-MHz NMR (VARIAN, UNITYNOVA-500 NMR). ^1H NMR spectra were also obtained in $d_6\text{-DMSO}$ and D_2O separately in a concentration of 0.5 wt % to characterize the structure of the amphiphilic micelles. The thermal properties were investigated by using differential scanning calorimetry (DSC) with a Thermal Analyzer 2920 at a heating rate of $10^{\circ}\text{C}/\text{min}$ under nitrogen.

Light Scattering and ζ -Potential Measurements. The effective hydrodynamic diameter of the micelles was measured at 25°C with a Zetasizer 3000ES (Malvern Instruments, Malvern, U.K.) and an argon laser beam of 670-nm wavelength with a detector angle of 90° . The

concentration of $\text{CS}_n\text{-PLLA}$ conjugates was kept constant at 1 mg/mL. The polydispersity index, μ_2/Γ^2 , was determined using the cumulant method. The measurements were averaged in triplicate.

Measurement of Critical Aggregation Concentration (CAC). The critical aggregation concentration was determined using pyrene as a fluorescence probe. Pyrene partitioned preferentially in the hydrophobic core of aggregates (micelles) and changed the photophysical properties of the micelles under investigation. Pyrene was first dissolved in acetone and then added to deionized water to a concentration of 5×10^{-7} M. Acetone was subsequently removed by reducing the pressure and stirring for more than 5 h at 30°C . The concentration of $\text{CS}_n\text{-PLLA}$ in the water was varied from 0.0001 to 0.1 g/L. The pyrene and $\text{CS}_n\text{-PLLA}$ in the water were conjugated and equilibrated at room temperature for 1 day before measurement. The fluorescence spectra were obtained at room temperature using a fluorescence spectrophotometer (Hitachi, F-2500). The fluorescence excitation spectra of pyrene were measured at a fixed emission wavelength (I_{em}) of 339 nm. The emission spectrum of pyrene was obtained at a fixed excitation wavelength (I_{ex}) of 390 nm.

Atomic Force Microscopy (AFM). Atomic force microscopy (AFM, SEIKO, SPA 400) experiments were performed in a tapping mode. A volume of $5\ \mu\text{L}$ of the micelle solution was dropped on a clear glass slide surface and air-dried at room temperature.

Fluorescence Labeling of Micelles. Flutamide was used as the fluorescence label for the $\text{CS}_n\text{-PLLA}$ micelles. It was incorporated into the micelles by a solvent evaporation method.

A 5-mg quantity of flutamide and 20 mg of copolymer were dissolved in dichloromethane. This solution was added to 50 mL of deionized water, and the mixture was stirred vigorously in an ice bath for 10 min. The organic solvent was removed by evaporation at reduced pressure. Dialysis was carried out to remove the unlabeled flutamide, and micelles were recovered by centrifugation at 30000 rpm for 30 min at 15°C .

Endocytosis of Micelles. The cellular uptake and distribution of fluorescence-labeled micelles in HS68 human fibroblast were examined by confocal microscopy (Axiovert 100 M). HS68 human fibroblasts were cultured in DMEM supplemented with 10% FBS, streptomycin at $100\ \mu\text{g}/\text{mL}$, penicillin at $100\ \text{IU}/\text{mL}$, and 2 mM L-glutamine. Cells were maintained at 37°C in a humidified 5% CO_2 atmosphere. An amount of 5×10^4 cells per well were seeded in a 24-well plate with slides in 2 mL of DMEM with 10% FBS. They were incubated for 24 h before further experiments were performed. After the medium had been replaced with fresh serum-free medium, the flutamide-labeled micellar aggregates were added at a concentration of $20\ \mu\text{g}/\text{mL}$. After various periods, the medium was discarded and the cells were washed several times with PBS. The cells were fixed by 4% glutaraldehyde (in PBS) followed by incubation at 4°C for 20 min. They were then washed with PBS, and the individual cover slides were mounted on clean glass slides and visualized with an Axiovert 100 M confocal

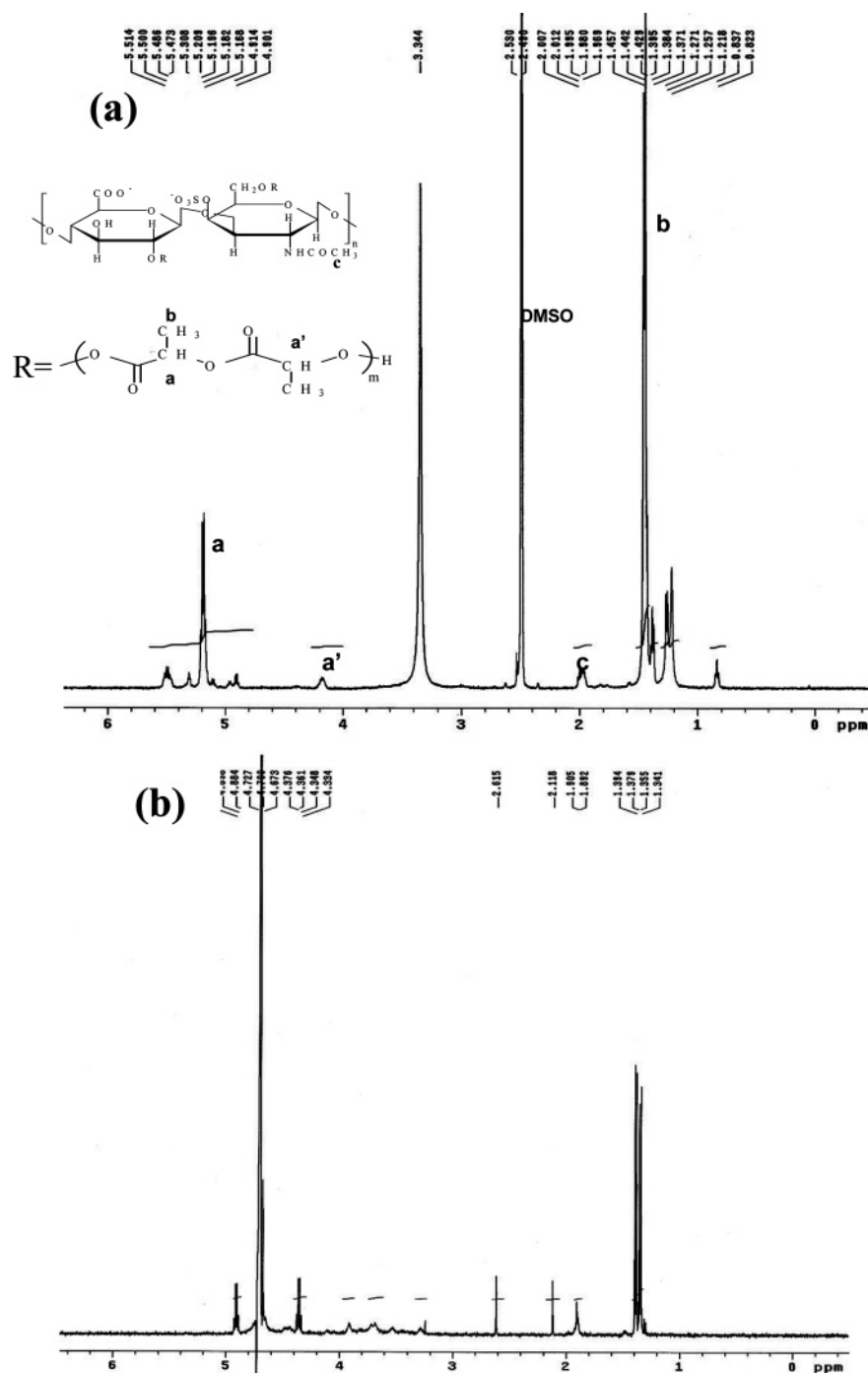


Figure 2. ¹H NMR spectroscopy of CS_{15.4}-PLLA nanoparticles in (a) d₆-DMSO and (b) D₂O.

microscope. A laser with an excitation line at 488 nm was used to introduce red fluorescence.

Results and Discussion

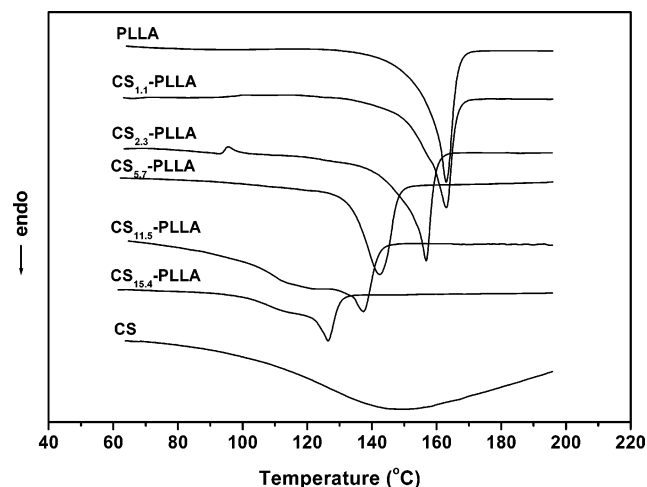
Synthesis of CS_n-PLLA Graft Copolymers. Preparation of the CS_n-PLLA graft copolymer was carried out according to Scheme 1. Chondroitin sulfate was grafted with L-lactide by ring-opening polymerization, and Sn(Oct)₂ was used as the catalyst. Figure 2a shows the representative ¹H NMR spectrum of the graft copolymer (CS_{15.4}-PLLA). The proton signals belonging to the $-\text{CH}$ or $-\text{CH}_2$ of disaccharide units in chondroitin sulfate are in the range 3–5 ppm, and the peak at 1.9 ppm corresponds to the methyl group. While the peak at 1.5 ppm with a doublet corresponds to the methyl group of the

PLLA moiety ($-\text{CH}(\text{CH}_3)\text{O}-\text{CO}-$), another peak at $\delta = 5.2$ ppm with a quartet is attributed to the internal methine proton of the PLLA ($-\text{CH}(\text{CH}_3)\text{O}-\text{CO}-$) and the peak at $\delta = 4.1$ ppm with a quartet belongs to the terminal methine proton of PLLA ($-\text{CH}(\text{CH}_3)\text{OH}$). The methine and methylene proton signals of the chondroitin sulfate observed at $\delta = 3$ and 5 ppm are extremely broad and weak because the content of chondroitin sulfate in the copolymer is very low and the mobility of the chondroitin sulfate in organic solvent is poor. The content of the chondroitin sulfate in the graft copolymer can also be described by the degree of substitution (DS) and the degree of polymerization (DP). The degree of substitution was calculated via ¹H NMR spectroscopy on the basis of the area ratio of signals from methine protons of PLLA segments at 5.2 ppm (H) and methyl proton of the chondroitin sulfate at 1.9 ppm

Table 1. Composition and Characterizations of CS_n-PLLA Conjugates

sample	feed ratio ^a	DS	DP	CS content ^b (%)	<i>d</i> ^c (nm)	μ_2/Γ^2 ^d	ζ^e (mV)	<i>K_v</i>
CS _{1.1} -PLLA	500	1.88	152.17	1.1	180 ± 5.2	0.1951	−18.3	N.D. ^f
CS _{2.3} -PLLA	400	1.42	94.10	2.3	163 ± 8.1	0.1192	−19.4	1.41 × 10 ⁶
CS _{5.7} -PLLA	200	1.18	44.27	5.7	149 ± 6.6	0.1485	−24.8	5.88 × 10 ⁵
CS _{11.5} -PLLA	100	1.12	21.45	11.5	127 ± 2.9	0.0957	−30.4	4.65 × 10 ⁵
CS _{15.4} -PLLA	50	1.08	15.75	15.4	92 ± 3.7	0.0961	−49.4	3.65 × 10 ⁵

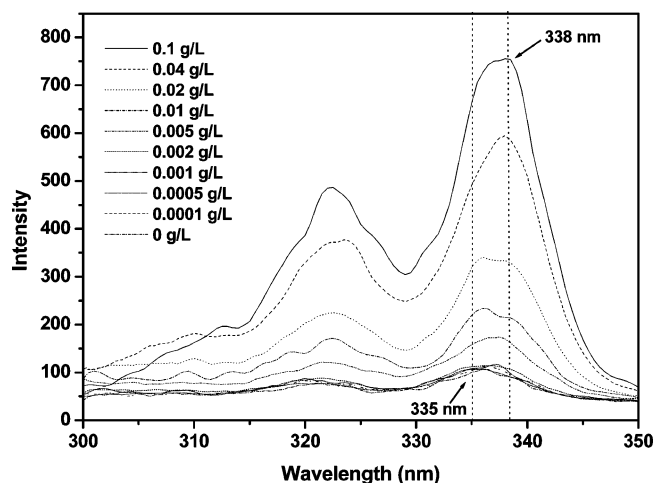
^a Feed ratio = PLLA/CS molar ratio. ^b Content of CS units in wt % = (chondroitin sulfate in g/grafted copolymer in g) × 100. ^c Mean diameter measured by dynamic light scattering with three different samples. ^d Polydispersity factors. ^e ζ -potential of the CS_n-PLLA conjugated in deionized water at 1 mg/mL. ^f N.D.: not determined.

**Figure 3.** DSC thermograms of CS, PLLA, and CS_n-PLLA with heating scans at 10 °C/min.

(3H) (Figure 2a). This value indicates the average numbers of the hydroxyl groups on the disaccharides of CS that have been reacted with L-lactide. The DS for these copolymers ranged from 1.08 to 1.88 (see Table 1). The degree of polymerization of L-lactide was also calculated using ¹H NMR spectroscopy on the basis of the area ratio of the terminal methine proton signal of PLLA at 4.1 ppm to the internal methine proton signal of PLLA segments at 5.2 ppm (see Table 1), which indicates the average length of every PLLA branch. The contents of CS in the copolymer were low, and the majority of the graft copolymers were PLLA.

To show the existence of the CS_n-PLLA graft copolymer, samples were analyzed by DSC. Figure 3 shows DSC heating scans of the graft copolymers and equivalent homopolymers of CS and PLLA. PLLA exhibits a sharp melting peak at 163 °C, and CS shows a broad endothermic peak. When the CS content in the copolymer increases, the melting temperature decreases gradually and the width of the peak becomes broader. The decrease in melting temperature should be a result of a change in the crystalline morphology of the PLLA segment: the lamellae become thinner and more imperfect as the content of CS increases in the copolymer. These thermograms also confirm that the PLLA is grafted onto the CS and only graft copolymer remains after purification as described in previous reports.^{18,19}

Formation of CS_n-PLLA Aggregation Micelles. To evidence the structure of the micelles in the aqueous media, the amphiphilic conjugate of CS_n-PLLA graft copolymer and the limited mobility of the PLLA chain in the core of the micelle were explicated via ¹H NMR spectra in different solvent systems, that is, *d*₆-DMSO and D₂O. As presented in Figure 2a, the copolymer is dissolved in *d*₆-DMSO, where micelle formation is not expected. Characteristic peaks of the protons

**Figure 4.** Excitation spectra of pyrene in the presence of an amphiphilic grafted copolymer at a fixed emission wavelength (*I_{em}*) of 390 nm. The concentration of pyrene was 5.0 × 10^{−7} M, and the graft copolymer concentration was varied from 0.0001 to 0.1 g/L.

of methyl groups, internal methine groups, and terminal methylene groups of PLLA are observed at 1.5, 5.2, and 4.1 ppm, respectively. However, when the micelles are dissolved in the D₂O (Figure 2b), these peaks disappear, indicating that the PLLA segments form a solid core which causes a broadening effect, due to the restricted proton mobility of PLLA chains, in the NMR spectroscopy. On the other hand, characteristic peaks of the protons of the chondroitin sulfate, belonging to the −CH or −CH₂ of the disaccharide units, are in the range 3–5 ppm while that of the methyl group appears at 1.9 ppm (Figure 2b). Thus, these results suggest that the amphiphilic grafted copolymer (CS_n-PLLA) aggregates can be reasonably considered to have a core–corona structure with chondroitin sulfate on the surface in an aqueous phase (Figure 1). This structure of CS_n-PLLA aggregates is similar to that of amphiphiles of low molecular weight and PEG-PLLA block copolymers.²⁰ These ¹H NMR spectra are consistent with other polymeric amphiphiles which form micelles in the aqueous phase.^{21–23}

Verification of Micelle Formation Using a Fluorescence Probe Technique. The formation of amphiphilic micelles in an aqueous phase and the critical aggregation concentration (CAC) for CS_n-PLLA micellar aggregates were confirmed by the fluorescence technique with pyrene as a fluorescence probe.²⁴ The fluorescence of pyrene is known to be sensitive to changes in the microenvironment.²⁵ When the micelles are formed in an aqueous phase, pyrene molecules are preferentially located within or close to the hydrophobic microdomain of the micelles. Consequently, the photophysical characteristics of pyrene molecules in a hydrophobic surrounding differ noticeably from those in an aqueous phase. Figure 4 shows the excitation spectra of pyrene in solutions of CS_n-PLLA with various concentrations.

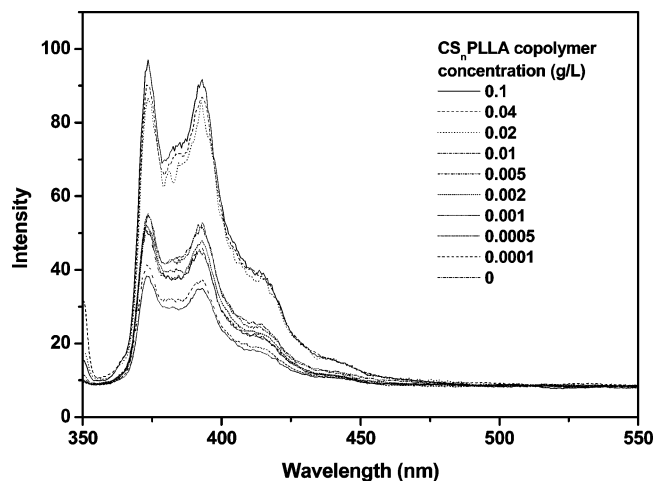


Figure 5. Fluorescence emission spectra of pyrene in the presence of CS_n-PLLA copolymer at a fixed excitation wavelength of 339 nm. The concentration of pyrene was 5.0×10^{-7} M, and the graft copolymer concentration was varied from 0.0001 to 0.1 g/L.

When the concentration is below the CAC (0.001 g/L), the total fluorescence intensity exhibits no significant change. However, the fluorescence intensity increases substantially with an increase of CS_n-PLLA concentration, indicating the formation of micelle and the incorporation of pyrene in the hydrophobic core of the micelle. The partition of pyrene causes the excitation peak of the (0,0) band to shift from 335 to 338 nm (red shift), which means that PLLA chains grafted on CS start to form hydrophobic domains and core–corona structure of the graft copolymer are formed in aqueous solution. The band change of pyrene is more sensitive to the critical micellization concentration than lifetime measurements or fluorescence emission changes. The transfer of pyrene from the polar environment to a nonpolar region significantly changes the intensity ratio of I_{338}/I_{335} due to the increase in the quantum yield of the fluorescence. Moreover, due to the difference in the local polarity (the Ham effect²⁶), the pyrene molecular emission spectrum varies with the formation of the polymeric micelle as well. Figure 5 shows the typical fluorescent emission spectra of pyrene in the presence of CS_n-PLLA micelles at a fixed excitation wavelength of 339 nm. The fluorescent emission spectra of pyrene in water exhibit five predominant peaks.²⁴ Pyrene is poorly soluble in water, but emits strongly when hydrophobic microdomains are formed in an aqueous solution, because it preferably lies close to (or inside) the hydrophobic microdomains.²⁷ The intensity of the third highest vibrational band as well as the total emission intensity of pyrene starts to increase drastically above a certain concentration (CAC) of CS_n-PLLA. In other words, the intensities of the emission spectra remain virtually constant below the CAC. As the concentration of the copolymer exceeds the CAC, the intensities of fluorescence increase substantially, suggesting the formation of micelles. Figure 6 plots the intensity ratio (I_{338}/I_{335}) for the pyrene excitation spectra versus the logarithm of CS_{2,3}-PLLA concentration. The apparent CAC was obtained from the crossover point in the low-concentration range. Thus, the CAC values for all CS_n-PLLA were in the range of 0.0043–0.0091 mg/mL, and they decreased with an increasing amount of hydrophobic segments (PLLA). The CAC, which is the threshold concentration of self-assembled formation by intra- or intermolecular association, was determined from the change of the intensity ratio (I_{338}/I_{335}) of the pyrene in the presence of the amphiphilic copolymer. The very low CAC values indicate a very strong tendency of the graft copolymers toward formation

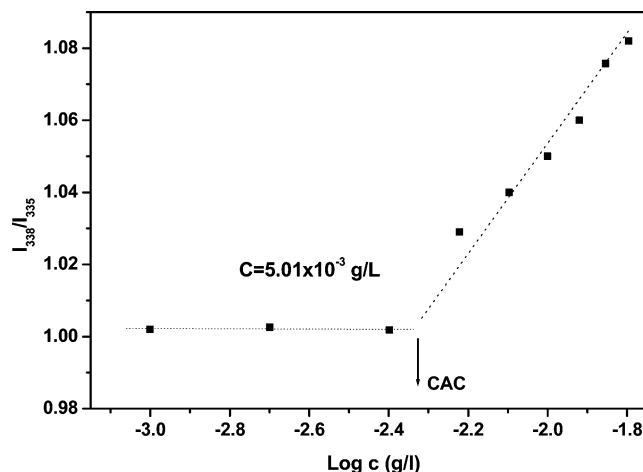


Figure 6. The intensity ratio of 338 nm/335 nm in the excitation spectra as a function of logarithm of the grafted copolymer concentration (CS_{2,3}-PLLA).

of micelles in aqueous solution.²⁸ The CAC of the micelles obtained in this investigation is similar to that of the poly(ethylene oxide)–poly(*b*-benzyl L-aspartate) copolymer micelle (CMC = 0.005–0.01 mg/mL),²⁹ but it is much lower than that of poloxamers (CMC = 1–24 mg/mL),³⁰ suggesting that this micelle is relatively stable. However, PLLA is a crystalline polymer which does not easily equilibrate at room temperature. Indeed, PLLA crystallites in the core of polymeric micelles are stabilized by strong van der Waals interactions and adopt a more compact conformation than enantiomeric crystals, allowing denser polymeric packing.³¹ To aid the system to attain equilibrium, it can be promoted by increasing the length of the hydrophobic segment,³¹ varying the solvent evaporation rate, reducing the preparation temperature,³² and so forth. On the basis of the preparative technique, the crystalline polymer in the core of the micelles should make it possible to reach equilibrium. The obtained structures are stable since their characteristics remain the same even after months, implying that thermodynamic equilibrium should be reached.

Partitioning of Pyrene in the Hydrophobic Core of Micelles. Hydrophobicity of the inner core of self-aggregated micelles is one important factor in its application as a drug carrier. In this study, the partition equilibrium constant (K_v) of pyrene in the hydrophobic core of micelles was estimated according to the method reported by Wilhelm et al.³³ and Lee et al.,³⁴ and it could be related to the hydrophobicity of the micellar core. The equilibrium constant K_v for partitioning of pyrene between the aqueous and micellar phases is one of the critical parameters related to micelle stability. Above CAC, the increase in signal due to the binding of pyrene becomes larger than the random error in determining the intensity of unbound component. This suggests that pyrene interacts with individual polymeric amphiphiles in a self-assembly, followed by partitioning into the inner core of the polymeric micelle. The binding of pyrene to micelles has been considered to be a simple equilibrium between the micellar phase and the water. The binding of pyrene to a micelle is assumed to result from the simple equilibrium between the micellar phase of volume (V_m) and the water phase of volume (V_w). Thus, the ratio of the concentration of pyrene in the micellar phase to that in the water phase ($[Py]_m/[Py]_w$) can be expressed as the ratio of the volumes of the two phases,

$$[Py]_m/[Py]_w = K_v V_m/V_w \quad (1)$$

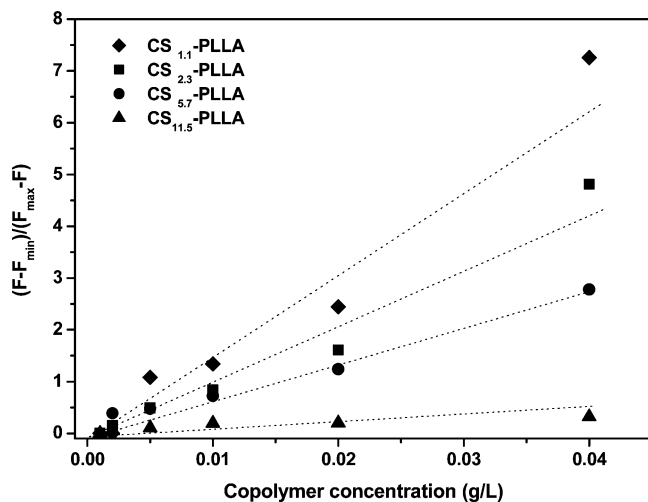


Figure 7. Plots of $(F - F_{\min})/(F_{\max} - F)$ vs copolymer concentration of $\text{CS}_n\text{-PLLA}$ in water.

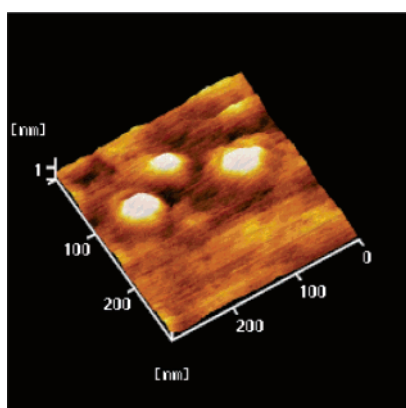


Figure 8. AFM image of $\text{CS}_{15.4}\text{-PLLA}$ nanoparticles on glass slide (topography).

The equation for the simple equilibrium of the pyrene in each phase can be rewritten as follows:

$$[\text{Py}]_{\text{m}}/[\text{Py}]_{\text{w}} = K_{\text{v}}x(\text{c-cac})/1000\rho \quad (2)$$

where x is the weight fraction of hydrophobic PLLA in the grafted copolymer and ρ is the density of the hydrophobic PLLA, which is assumed to be the value of the bulk poly(L-lactide) ($=1.248 \text{ g/mL}$).

When the polymer concentration exceeds the CAC, the ratio of fluorescent intensity $I_{338 \text{ nm}}/I_{335 \text{ nm}}$ increases dramatically. Hence, $[\text{Py}]_{\text{m}}/[\text{Py}]_{\text{w}}$ can be written as

$$[\text{Py}]_{\text{m}}/[\text{Py}]_{\text{w}} = (F - F_{\min})/(F_{\max} - F) \quad (3)$$

where F_{\max} and F_{\min} are the average intensity ratios $I_{338 \text{ nm}}/I_{335 \text{ nm}}$ in the regions of low and high polymer concentrations, respectively, and F is the intensity ratio $I_{338 \text{ nm}}/I_{335 \text{ nm}}$ in the intermediate polymer concentration region.

Combining eqs 2 and 3 yields

$$(F - F_{\min})/(F_{\max} - F) = K_{\text{v}}x(\text{c-cac})/1000\rho \quad (4)$$

where the K_{v} values of pyrene can be determined using a plot of $(F - F_{\min})/(F_{\max} - F)$ versus the copolymer concentration (as shown in Figure 7).

Table 1 summarizes the K_{v} values for graft copolymers, and they are between 3.65×10^5 and 1.41×10^6 . As shown in Table 1, K_{v} increases with increasing PLLA content in the copolymer, indicating the increase of hydrophobicity of the micelles. The K_{v} values of the $\text{CS}_n\text{-PLLA}$ micelles are in the same order as those of other micelles ($\sim 10^5$),²² revealing similar hydrophobicities in these micellar cores.

DLS and Morphology Observation. The hydrodynamic volume and the polydispersity factor (μ_2/Γ^2) of the micelles were estimated by dynamic light scattering (DLS). The sizes of amphiphilic core (PLLA)–corona (CS) micelles, with different CS content, were all smaller than 200 nm (Table 1). The results indicate that the mean diameter increases as the hydrophobic segment (PLLA) content in the copolymer increases, because CS (hydrophilic segment) has uniform chain length. The polydispersity factors for all micelles of different compositions are fairly low (below 0.2) (Table 1). The hydrodynamic radius and the size distribution from dynamic light scattering show a clear self-assembly of copolymers because the hydrodynamic radius is larger than that of a single chain. However, the fact that the size of the aggregates is always larger than that of a single micelle should be due to the formation of a compound micelle.³⁵ For all these copolymers, only very narrowly distributed particles were observed, implying they were well-defined, presumably micelle-like core–shell nanostructures, with the insoluble PLLA as the core and the soluble CS as the shell.³⁶ Additionally, the surfaces of the micelles were negatively charged, as reflected by the ζ -potential values (Table 1) which depended on the composition of the micelles. It is obvious that

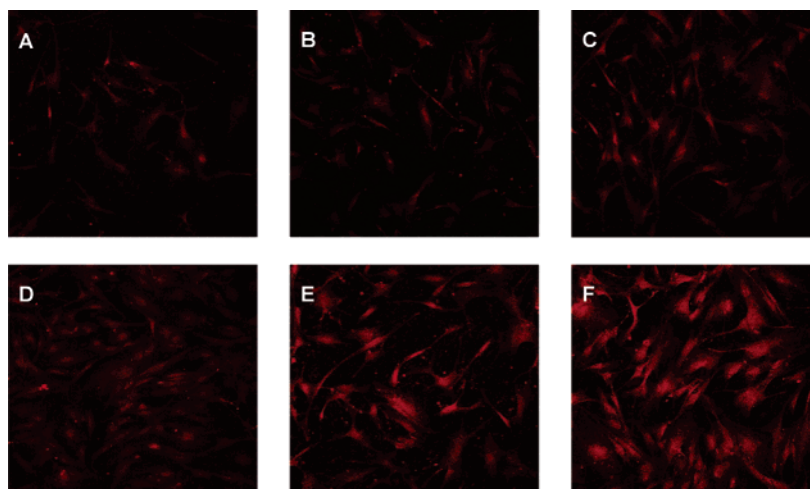


Figure 9. Confocal images of cellular uptake of flutamide-loaded aggregates transported into HS68 human fibroblast cells for different time intervals: (A) 1 h, (B) 2 h, (C) 4 h, (D) 6 h, (E) 8 h, and (F) free flutamide for 4 h. The concentration of the polymeric aggregates was $20 \mu\text{g/mL}$.

the large negative ζ -potential of CS_n-PLLA aggregates is attributed to the presence of ionized carboxyl groups and sulfonic acid groups on the micellar surface, which indicates that negatively charged chondroitin sulfate covers the self-aggregates. Copolymer CS_{1.1}-PLLA shows the lowest negative ζ -potential because it has the fewest carboxyl groups and sulfonic acid groups on the surface of the micelles. Atomic force microscopy was also used to visualize directly the size and the morphology of the micelles. Figure 8 demonstrates that the micelles of CS_{15.4}-PLLA were spherical with an average diameter of 85 nm. The morphological characteristics of the polymeric micelles were quite similar to those of other reported synthetic micelles.³⁷ The diameters of the micelles shown in the AFM image are slightly smaller than those obtained from DLS measurements, perhaps because water was removed from the micelles in AFM observation. Additional AFM images confirmed the narrow size distribution of the micelles.

Cell Uptake and Distribution Studies. To visualize the effect of internalization of the CS_n-PLLA micelles into cells, the intracellular distribution of the micelles in cells was investigated by laser confocal microscopy. Flutamide-loaded micellar aggregates were employed to elucidate the internalization process of CS_n-PLLA micelles into cells. HS68 human fibroblast cells readily take up these micelles, as shown in Figure 9. The fluorescence-labeled micelles are distributed over the intracellular space of the cytoplasm. Very few administered micelles were present in the washing medium, so a large proportion of the administered micelles were internalized by the cells through nonspecific endocytosis. After 4 h, the fluorescence image revealed a high concentration of micelles localized in the cytoplasm and in the perinuclear region. The rate of absorption is governed by the concentration gradient across the cells. Furthermore, washing the cells with phosphate-buffered saline did not eliminate the fluorescence, possibly binding of the dye with an intracellular component. Confocal microscopic observations demonstrate that CS_n-PLLA micelles can transport effectively within cells. In previous literature, it has been found that the presence of a negative charge at the surface of the micelle will enhance the extent of in-vitro uptake into cells.³⁸ The amount of micelles transported increases with time. Flutamide (without micelle encapsulation) transports into cells more quickly (less than 4 h) because of its smaller size. In the meantime, internalization also delays the transportation of the micelles.

Conclusions

In this study, amphiphilic graft copolymers with a backbone of chondroitin sulfate and side chains of poly(L-lactide) were prepared. Chondroitin sulfate was used as the macroinitiator, allowing the number of grafting points and the length of the side chain to be controlled by feed composition. ¹H NMR in D₂O provided evidence of the formation of micelles of CS_n-PLLA graft copolymers and the limited mobility of the PLLA chains in the core of the micelles. Fluorescence excitation spectra revealed the formation of hydrophobic domains and were used to obtain the critical aggregation concentration (CAC). The CAC values of CS_n-PLLA graft copolymers depend on the content of hydrophobic segments and are in the range of 0.0043–0.0091 mg/mL. The *K_v* values of the micelles with different CS contents were obtained by fluorescence. The analysis of aggregation behavior due to the association of the hydrophobic segments provides useful information about the structure and physicochemical properties of micelles for developing a delivery device.

The mean diameters of the self-aggregated micelles were less than 200 nm with narrow size distribution, and the spherical shape was observed by AFM. Confocal scanning microscopy revealed that the uptake of micelles inside the cell membrane was significant. Such a graft copolymer conjugate, with an outer shell of chondroitin sulfate, has potential for bioadhesion to mucosa surfaces in the colon.

Acknowledgment. This research was supported by Ministry of Economic Affairs, Taiwan, ROC, under Technology Development Program for Academia Grant 93-EC-17-A-17-S1-0009.

References and Notes

- (1) Gaucher, G.; Dufresne, M. H.; Sant, V. P.; Kang, N.; Maysinger, D.; Leroux, J. C. Block copolymer micelles: Preparation, characterization and application in drug delivery. *J. Controlled Release* **2005**, *109*, 169–188.
- (2) Rösler, A.; Vandermeulen, G. W. M.; Klok, H. A. Advanced drug delivery devices via self-assembly of amphiphilic block copolymer. *Adv. Drug Delivery Rev.* **2001**, *53*, 95–108.
- (3) Kwon, G. S.; Okano, T. Polymeric micelles as new drug carriers. *Adv. Drug Delivery Rev.* **1996**, *21*, 107–116.
- (4) Rosler, A.; Vandermeulen, G. W. M.; Klok, H. A. Advanced drug delivery devices via self-assembly of amphiphilic block copolymers. *Adv. Drug Delivery Rev.* **2001**, *53*, 95–108.
- (5) Taubert, A.; Napoli, A.; Meier, W. Self-assembly of reactive amphiphilic block copolymers as mimetics for biological membranes. *Curr. Opin. Chem. Biol.* **2004**, *8*, 598–603.
- (6) Miralles-Houzelle, M. C.; Hubert, P.; Dellacherie, E. Hydrophobic alkyl chains-pectin conjugates. Comparative study of some physicochemical properties in relation to covalent coupling vs ionic association. *Langmuir* **2001**, *17*, 1384–1391.
- (7) Hou, S.; Chaikof, E. L.; Tatou, D.; Gnanou, Y. Synthesis of water-soluble star-block and dendrimer-like copolymers based on poly(ethylene oxide) and poly(acrylic acid). *Macromolecules* **2003**, *36*, 3874–3881.
- (8) Kang, H. S.; Yang, S. R.; Kim, J. D.; Han, S. H.; Chang, I. S. Effect of grafted alkyl groups on aggregation behavior of amphiphilic poly(aspartic acid). *Langmuir* **2001**, *17*, 7501–7506.
- (9) Inoue, T.; Chen, G.; Nakamae, K.; Hoffman, A. S. An AB block copolymer of oligo(methyl methacrylate) and poly(acrylic acid) for micellar delivery of hydrophobic drugs. *J. Controlled Release* **1998**, *51*, 221–229.
- (10) Lee, S. C.; Chang, Y.; Yoon, J. S.; Kim, C.; Kwon, I. C.; Kim, Y. H.; Jeong, S. Y. Synthesis and micellar characterization of amphiphilic diblock copolymers based on poly(2-ethyl-2-oxazoline) and aliphatic polyesters. *Macromolecules* **1999**, *32*, 1847–1852.
- (11) Jeong, J. H.; Park, T. G. Novel polymer-DNA hybrid polymeric micelles composed of hydrophobic poly(D,L-lactide-co-glycolic acid) and hydrophilic oligonucleotides. *Bioconjugate Chem.* **2001**, *12*, 917–923.
- (12) Kwon, G. S.; Okano, T. Polymeric micelle as new drug carriers. *Adv. Drug Delivery Rev.* **1996**, *21*, 107–116.
- (13) Nah, J. W.; Jeong, Y. I.; Cho, C. S. Polymeric micelle formation of multiblock copolymer composed of poly(γ -benzyl L-glutamate) and poly(ethylene oxide). *Bull. Korean Chem. Soc.* **2000**, *21*, 383–388.
- (14) Soppimath, K. S.; Aminabhavi, T. M.; Kulkarni, A. R.; Rudzinski, W. E. Biodegradable polymeric nanoparticles as drug delivery devices. *J. Controlled Release* **2001**, *70*, 1–20.
- (15) Marie, E.; Landfester, K.; Antonietti, M. Synthesis of chitosan-stabilized polymer dispersions, capsules, and chitosan grafting products via miniemulsion. *Biomacromolecules* **2002**, *3*, 475–481.
- (16) Erlich, R. B.; Werneck, C. C.; Mourao, P. A. S. Major glycosaminoglycan species in the developing retina: synthesis, tissue distribution and effects upon cell death. *Exp. Eye Res.* **2003**, *77*, 157–165.
- (17) Pieper, J. S.; van Wachem, P. B.; van Luyn, M. J. A.; Brouwer, L. A.; Hafmans, T.; Veerkamp, J. H.; van Kuppevelt, T. H. Attachment of glycosaminoglycans to collagenous matrixes modulates the tissue response in rats. *Biomaterials* **2000**, *21*, 1689–1699.
- (18) Donabedian, D. H.; McCarthy, S. P. Acrylation of pullulan by ring opening of lactones. *Macromolecules* **1998**, *31*, 1032–1039.
- (19) Chen, L.; Qui, X.; Deng, M.; Hong, Z.; Luo, R.; Chen, X.; Jing, X. The starch grafted poly(L-lactide) and the physical properties of its blending composites. *Polymer* **2005**, *46*, 5723–5729.

- (20) Nagasaki, Y.; Okada, T.; Scholz, C.; Iijima, M.; Kato, M.; Kataoka, K. The reactive polymeric micelle based on an aldehyde-ended poly(ethylene glycol)/poly(lactide) block copolymer. *Macromolecules* **1998**, *31*, 1473–1479.
- (21) Kwon, S.; Park, J. H.; Chung, H.; Kwon, I. C.; Jeong, S. Y. Physicochemical characteristics of self-assembled nanoparticles based on glycol chitosan bearing 5 β -cholanolic acid. *Langmuir* **2003**, *19*, 10188–10193.
- (22) Kim, C.; Lee, S. C.; Kang, S. W.; Kwon, I. C.; Kim, Y. H.; Jeong, S. Y. Synthesis and the micellar characteristics of poly(ethylene oxide)-deoxycholic acid conjugates. *Langmuir* **2000**, *16*, 4792–4797.
- (23) Park, K.; Kim, K.; Kwon, I. C.; Kim, S. K.; Lee, S.; Lee, D. Y.; Byun, Y. Preparation and characterization of self-assembled nanoparticles of heparin-deoxycholic acid conjugates. *Langmuir* **2004**, *20*, 11726–11731.
- (24) Kalyanasundaram, K.; Thomas, J. K. Environment effects on vibronic band intensities in pyrene monomer fluorescence and their application in studies of micellar system. *J. Am. Chem. Soc.* **1997**, *99*, 22039–22044.
- (25) Ananthapadamanabhan, K. P.; Goddard, E. D.; Turro, N. J.; Kuo, P. L. Fluorescence probes for critical micelle concentration. *Langmuir* **1985**, *1*, 352–355.
- (26) Zhao, C.; Winnik, M. A.; Riess, G.; Croucher, M. D. Fluorescence probe techniques used to study micelle formation in water-soluble block copolymers. *Langmuir* **1990**, *6*, 514–516.
- (27) Astafieva, I.; Zhong, X. F.; Eisenberg, A. Critical micellization phenomena in block polyelectrolyte solutions. *Macromolecules* **1993**, *26*, 7339–7352.
- (28) Lele, B. S.; Leroux, J. C. Synthesis and micellar characterization of novel amphiphilic A-B-A triblock copolymers of *N*-(2-hydroxypropyl)methacrylamide or *N*-vinyl-2-pyrrolidone with poly(ϵ -caprolactone). *Macromolecules* **2002**, *35*, 6714–6723.
- (29) Kwon, G.; Naito, M.; Yokoyama, M.; Okano, T.; Sakurai, Y.; Kataoka, K. Micelles based on AB block copolymers of poly(ethylene oxide) and poly(*b*-benzyl L-aspartate). *Langmuir* **1993**, *9*, 945–949.
- (30) Prasad, K. N.; Luong, T. T.; Florence, A. T.; Paris, J.; Vautin, C.; Seiller, M.; Puisieux, F. Surface activity and association of ABA polyoxyethylene-polyoxypropylene block copolymers in aqueous solution. *J. Colloid Interface Sci.* **1982**, *90*, 303–309.
- (31) Kang, N.; Perron, M. E.; Prud'homme, R. E.; Zhang, Y.; Gaucher, G.; Leroux, J. C. Stereocomplex block copolymer micelle: core-shell nanostructures with enhanced stability. *Nano Lett.* **2005**, *5*, 315–319.
- (32) Portinha, D.; Bouteiller, L.; Pensec, S.; Richez, A. Influence of preparation conditions on the self-assembly by stereocomplexation of polylactide containing diblock copolymers. *Macromolecules* **2004**, *37*, 3401–3406.
- (33) Wilhelm, M.; Zhao, C. L.; Wang, Y.; Xu, R.; Winnik, M. A.; Mura, J. L.; Riess, G.; Croucher, M. D. Poly(styrene-ethylene oxide) block copolymer micelle formation in water: a fluorescence probe study. *Macromolecules* **1991**, *24*, 1033–1040.
- (34) Lee, S. C.; Chang, Y.; Yoon, J. S.; Kim, C.; Kwon, I. C.; Kim, Y. H.; Jeong, S. Y. Synthesis and micellar characterization of amphiphilic diblock copolymers based on poly(2-ethyl-2-oxazoline) and aliphatic polyesters. *Macromolecules* **1999**, *32*, 1847–1852.
- (35) Yu, K.; Eisenberg, A. Multiple morphology in aqueous solutions of aggregates of polystyrene-*block*-poly(ethylene oxide) diblock copolymers. *Macromolecules* **1996**, *29*, 6359–6361.
- (36) Tu, Y.; Wan, X.; Zhang, H.; Fan, X.; Chen, X.; Zhou, Q. F.; Chau, K. Self-assembly nanostructures of rod-coil diblock copolymers with different rod lengths. *Macromolecules* **2003**, *36*, 6565–6569.
- (37) Liu, M.; Dong, J.; Yang, Y.; Yang, X.; Xu, H. Characterization and release of triptolide-loaded poly(D,L-lactic acid) nanoparticles. *Eur. Polym. J.* **2005**, *41*, 375–382.
- (38) Eisenberg, A.; Allen, C.; Maysinger, D. Nano-engineering block copolymer aggregates for drug delivery. *Colloids Surf. B: Biointerfaces* **1999**, *16*, 3–27.

BM050995J